18th Brazilian Congress of Thermal Sciences and Engineering
November 16-20, 2020 (Online)

ENC-2020-0253
LAMINAR COFLOWING JETS FLAMES INSIDE TUBES WITH IRREGULAR WALLS

Rafael J. Leitão
Ricardo L. Soares Júnior
Albino J. K. Leiroz
Department of Mechanical Engineering – POLI/ COPPE
Federal University of Rio de Janeiro - UFRJ
PO Box 68503, Rio de Janeiro, Rio de Janeiro 21941-972, Brazil
rafajapi@poli.ufrj.br, riclsoaresjr@mecanica.coppe.ufrj.br, leiroz@mecanica.coppe.ufrj.br

Abstract. *Irregular surfaces are often present in a wide variety of heat transfer applications where equipment compactness is sought. The presence of irregularities or rough elements also disturbs the flow field near the solid surfaces changing the heat transfer rate. In the present study, axisymmetric confined reactive flows within cylindrical tubes with wall irregularities are analyzed. The reactive flow is described by the classical Shvab-Zeldovich formulation for unitary Lewis number. The mathematical model is based on mass, momentum, and mixture fraction conservation equations and considers the Burke-Schumann reaction mechanism and ideal gas behavior. Temperature dependence of the thermophysical properties is considered in the model. The Finite Volume Method is employed to discretize the governing equations, with a collocated grid arrangement. The SIMPLEC algorithm is employed to address the pressure-velocity coupling. A parametric study is conducted to evaluate the effects on the recirculation zones and the flame shape of the position and the size of the irregularities, of buoyancy and of the Reynolds number of the fluid flow. The shape and high of the flame are strongly affected by the changes in the wall irregularities as well as the recirculation zones besides the Reynolds number modifications drive changes in the flame behavior.*
.
Keywords: *Irregular Surface, Diffusion Flame, Flame Sheet Model, Finite Volume Method.*

1. INTRODUCTION

Diffusion flames play an important role in practical combustion applications. The term diffusion flame was applied by Burke and Schumann (1928) to designate flames in which fuel and oxidant are initially separated and mixing occurs in a region where combustion occurs, forming a flame structure. Although in practical applications are usually subject to turbulent flow, laminar diffusion flames provide the basic component for flamelet model, in which the structure of turbulent diffusion flames are interpreted as a composition of a set of laminar diffusion flames (García et al, 2020).

Studies of confined flames in channels are important due to application in fire tube boilers (Ortiz, 2011) and tube firing burners. Most studies of diffusion flames in the presence of irregular walls are related to flame holders, for which the solid wall is located downstream of the flame (Nascimento, 2005), as in the flame holders. Flame/wall interaction, for example, is a field of combustion that has not been investigated yet with sufficient care (Shilong and Yuxin, 2020).

Flame holders like bluff-body and cavity are an effective strategy to anchor the flame owing the recirculation zone. Despite, the flame holder cannot significantly extend the flammability limit of the mixture, heat recirculation is commonly used as method to broaden the flammable range based on equivalence ratio (Wan et al, 2020). The thermal condition of flame holder and combustion chamber wall and their interaction on flame stabilization was investigated (Wan and Zhao, 2020). Ansari and Amani (2018) found that the flame can be well anchored by the cylindrical bluff-body flame holder in a micro plate combustor. The bluff-body ball also had a significant effect on improving the flame stabilization of methane/air premixed mixture (Pan et al, 2020).

In the present study, the chemical reaction terms in the conservation equations are treated by the classical Shvab-Zeldovich formulation for unitary Lewis number. Single step, infinitely fast chemical reaction is considered, making possible to combine species conservation and energy conservation equations, and defining the flame locus under the hypothesis of infinitely thin flame. The wall irregularities are placed alongside the flame allowing for interaction between the reaction sheet and the irregular boundary. Effects on flame height and shape are evaluated. A parametric study is conducted to evaluate the effects on the recirculation zones and the flame shape of the position and the size of the irregularities, of buoyancy and of the Reynolds number of the fluid flow.

2. MATHEMATICAL MODEL

A sketch of the physical domain is shown in Fig. 1. The physical domain consists of two concentric circular tubes where fuel and oxidizer are injected through the inner and annular space, respectively. On the inlet, fuel and oxidizer velocity profiles are considered uniform but not necessarily equal. It is also considered adiabatic conditions for the annular space tube and atmospheric pressure on the outlet of the burner. At an arbitrary position, there is a region where the domain suffers constrictions and expansions to return to its original diameter.

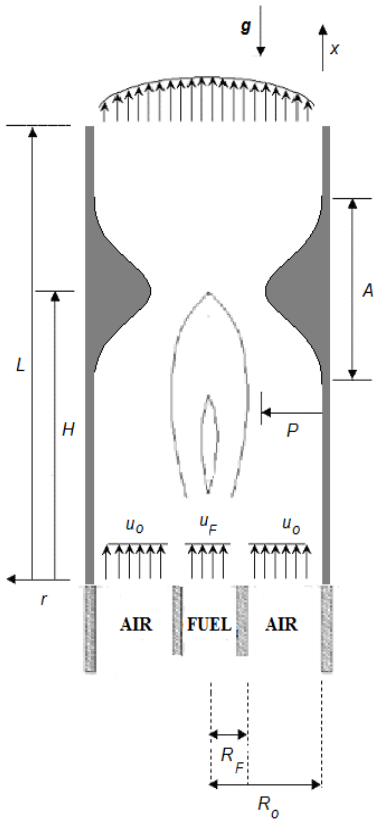

Figure. 1. Representative model of the physical problem.

The reactive flows in multicomponent systems are governed by three laws of conservation, they are: mass conservation, momentum conservation and energy conservation. These conservation laws can be mathematically written as the equation of continuity, equation of moment, equation of energy and equation of chemical species.

In order to simplify this set of equations, the heat flux due the radiation effects is neglected. This simplification is done because of the low absorptivity of the gases used in the present study. To further simplify the governing equations it is assumed that the dissipation by viscous stress and the flow work is negligible as well as the Soret e Dufour effects. Besides, the specific heat is considered constant for all chemical species and the diffusion velocity obey the Fick's law.

The flame sheet model, first introduced in (Burke and Schumann, 1928), makes the hypothesis that the chemical reaction is confined in a thin reaction zone where fuel and oxidizer cannot coexist, this assumption results in the absence of oxidizer in the fuel side and of fuel in the oxidizer side. Fuel and oxidizer flow towards the reaction zone in stoichiometric proportions, this condition becomes necessary in order to the reactants be completely consumed. In this model, the chemical reactions are described by a single one-step irreversible reaction corresponding in an infinitely fast conversion of reactants into stable products, as Eq. (1).

$$\nu_F \mathrm{F} + \nu_O \mathrm{O}_2 + \nu_N \mathrm{N}_2 \rightarrow \nu_P \mathrm{P} + \nu_N \mathrm{N}_2 \tag{1}$$

where ν is the stoichiometric coefficient, *F* is the fuel and *P* is the product. The nitrogen is considered an inert gas in this reaction.

The equations of chemical species and energy can be linearly combined in order to eliminate the reaction terms. Thus, a chemistry-free conservation equation, Eq. (5), can be written in terms of mixture fraction.

The reactive flow governing equations are written, in the cylindrical axisymmetric coordinate system, as

$$\frac{\partial \rho}{\partial t}+\frac{1}{r}\frac{\partial}{\partial x}\left(\rho r u\right)+\frac{1}{r}\frac{\partial}{\partial r}\left(\rho r v\right)=0 \tag{2}$$

$$\begin{aligned}&\frac{\partial}{\partial t}\left(\rho u\right)+\frac{1}{r}\frac{\partial}{\partial x}\left(\rho r u u\right)+\frac{1}{r}\frac{\partial}{\partial r}\left(\rho r u v\right)=-\frac{\partial p}{\partial x}+\frac{1}{r}\frac{\partial}{\partial x}\left(r\mu\frac{\partial u}{\partial x}\right)+\\&+\frac{1}{r}\frac{\partial}{\partial r}\left(r\mu\frac{\partial u}{\partial r}\right)+\frac{1}{r}\frac{\partial}{\partial r}\left(r\mu\frac{\partial v}{\partial x}\right)+\frac{1}{3}\frac{1}{r}\frac{\partial}{\partial x}\left(r\mu\frac{\partial u}{\partial x}\right)-\frac{2}{3}\frac{1}{r}\frac{\partial}{\partial x}\left[\mu\frac{\partial\left(rv\right)}{\partial x}\right]+\rho g\end{aligned} \tag{3}$$

$$\begin{aligned}&\frac{\partial}{\partial t}\left(\rho v\right)+\frac{1}{r}\frac{\partial}{\partial x}\left(\rho r u v\right)+\frac{1}{r}\frac{\partial}{\partial r}\left(\rho r v v\right)=-\frac{\partial p}{\partial r}+\frac{1}{r}\frac{\partial}{\partial x}\left(r\mu\frac{\partial v}{\partial x}\right)+\frac{1}{r}\frac{\partial}{\partial r}\left(r\mu\frac{\partial v}{\partial r}\right)+\frac{1}{r}\frac{\partial}{\partial r}\left(r\mu\frac{\partial v}{\partial r}\right)+\\&+\frac{1}{r}\frac{\partial}{\partial x}\left(r\mu\frac{\partial u}{\partial x}\right)-\frac{2}{3}\frac{1}{r}\frac{\partial}{\partial r}\left[\mu\frac{\partial\left(rv\right)}{\partial x}\right]-\frac{2}{3}\frac{1}{r}\frac{\partial}{\partial r}\left[\mu\frac{\partial u}{\partial x}\right]-\frac{2\mu}{r^2}+\frac{2}{3}\frac{\mu}{r^2}\frac{\partial}{\partial r}\left(rv\right)+\frac{2}{3}\frac{\mu}{r}\frac{\partial u}{\partial x}\end{aligned} \tag{4}$$

$$\frac{\partial}{\partial t}\left(\rho Z\right)+\frac{1}{r}\frac{\partial}{\partial x}\left(\rho r u Z\right)+\frac{1}{r}\frac{\partial}{\partial r}\left(\rho r v Z\right)-\left\{\frac{1}{r}\frac{\partial}{\partial x}\left[\rho r D\frac{\partial Z}{\partial x}\right]+\frac{1}{r}\frac{\partial}{\partial r}\left[\rho r D\frac{\partial Z}{\partial r}\right]\right\}=0 \tag{5}$$

where x and r are axial and radial coordinates, t is time, u e v are axial and radial velocities, ρ and μ are the density and dynamic viscosity of the mixture, p is pressure, g is gravitational acceleration, D is mass diffusivity of the mixture and Z is mixture fraction.

Denoting the variables at the flame surface with the subscript f, it can be shown that the mixture fraction at the flame Z_f can be given by (Willian, 1965):

$$Z_f=\left(1+\frac{sY_{FF_i}}{Y_{OA_i}}\right)^{-1} \tag{6}$$

where Y is the mass fraction, the subscripts F_i and A_i denote the condition in the inlet of the inner and outer tube, respectively, and s represents the stoichiometric mass coefficient.

With the formulation for the mixture fraction Z, it is possible to obtain the temperature profile and the mass fraction of the chemical species from the solution of Eqs. (2)-(5).

On the fuel side of the flame, the Eqs. (7)-(11) are used for determination of temperature and chemical species fields:

$$T=ZT_{F_i}+\left(T_{A_i}+Y_{OA_i}-\frac{h_{RP}}{c_p}\right)\left(1-Z\right) \tag{7}$$

$$Y_F=ZY_{FF_i}+Y_{OA_i}\frac{W_F\nu_F}{W_O s}\left(1-Z\right) \tag{8}$$

$$Y_O=0 \tag{9}$$

$$Y_P=Y_{OA_i}\frac{W_P\nu_P}{W_O s}\left(1-Z\right) \tag{10}$$

$$Y_N=Y_{NA_i}\left(1-Z\right)+ZY_{NF_i} \tag{11}$$

and on the oxidizer side:

$$T = \left(1-Z\right)T_{A_i} + \left(T_{F_i} + Y_{FA_i} - \frac{h_{RP}}{c_p}\right)Z \tag{12}$$

$$Y_F = 0 \tag{13}$$

$$Y_O = \left(Z-1\right)Y_{OA_i} - Y_{FF_i}\frac{W_O\nu_O}{W_F\nu_F}Z \tag{14}$$

$$Y_P = Y_{FF_i}\frac{W_P\nu_P}{W_F\nu_F}Z \tag{15}$$

$$Y_N = Y_{NA_i}\left(1-Z\right) + ZY_{NF_i} \tag{16}$$

where T is temperature, W is molecular weight of each specie, c_p is specific heat at constant pressure in mass unit and h_{RP} is enthalpy of reaction.

In the case of two products, as Eq. (17):

$$\nu_F \mathrm{F} + \nu_O \mathrm{O}_2 + \nu_N \mathrm{N}_2 \rightarrow \nu_{P_1}\mathrm{P}_1 + \nu_{P_2}\mathrm{P}_2 + \nu_N \mathrm{N}_2 \tag{17}$$

The species profiles Y_{P1} e Y_{P2} are given by:

$$Y_{P_1} = \left(\frac{W_{P_1}\nu_{P_1}}{W_{P_1}\nu_{P_1} + W_{P_2}\nu_{P_2}}\right)Y_P \tag{18}$$

$$Y_{P_2} = \left(\frac{W_{P_2}\nu_{P_2}}{W_{P_1}\nu_{P_1} + W_{P_2}\nu_{P_2}}\right)Y_P \tag{19}$$

Temperature variation of the thermophysical properties and transport coefficients is given by the Eqs. (20)-(22):

$$\rho = \frac{pW_{mix}}{T\,R_u} \tag{20}$$

$$\rho D = \frac{\mu}{Pr_{ref}} \tag{21}$$

$$\mu = \mu_{ref}\left(\frac{T}{T_{ref}}\right)^{\gamma} \tag{22}$$

where W_{mix} is the molecular weight of the mixture, $R_u = 8.314\ J\cdot K^{-1}\cdot mol^{-1}$ is the universal gas constant, $\gamma = 0.7$, $T_{ref} = 298\ K$ and $\mu_{ref} = 1.85\cdot 10^{-4}\ g/cm\cdot s$ are reference values for air (Kanury, 1982).

The heat generation parameter h_{RP}/c_P is given by an estimated value for the flame experimental temperature T_f, according to the Eq. (23):

$$-\frac{h_{RP}}{c_p} = \frac{1}{Y_{FF_i}}\left[\frac{T_f - T_{A_i}\left(1-Z_f\right)}{Z_f} - T_{F_i}\right] \tag{23}$$

For a methane-air flame, $T_f = 2050\ K$ (Xu and Smooke, 1993).

The governing equations (2)-(5) are subject to the following boundary conditions:

$$\frac{\partial u}{\partial r} = v = \frac{\partial Z}{\partial r} = 0 \quad @ 0 < x < L \,, r = 0 \tag{24}$$

$$\frac{\partial u}{\partial x} = \frac{\partial v}{\partial x} = \frac{\partial Z}{\partial x} = 0 \,,\; p = p_a \quad @ x = L \,, 0 < r < R_O \tag{25}$$

$$u = u_F \,,\; v = 0 \,,\; Z = 1 \quad @ \; x = 0 \,, 0 < r < R_F \tag{26}$$

$$u = u_O \,,\; v = 0 \,, \quad Z = 0 \quad @ x = 0 \,, R_F < r < R_O \tag{27}$$

$$\boldsymbol{v} \bullet \boldsymbol{n} = \boldsymbol{v} \bullet \boldsymbol{t} = \frac{\partial Z}{\partial \boldsymbol{n}} = 0 \quad @ 0 < x < L \,, r = R_w(x) \tag{28}$$

where p_a is the atmospheric pressure, $\boldsymbol{n}$ and $\boldsymbol{t}$ are the normal and tangential vectors to the solid wall, respectively. A Gaussian function $R_w(x)$ models the wavy wall as:

$$R_w(x) = R_O - Pe^{\frac{-(x-H)^2}{\sigma}} \tag{29}$$

where, as exposed in Fig. 1, H is the axial position of the wavy wall peak, P controls its radial position, σ controls the width of the wavy wall and $e \approx 2.718$ is the Euler's number.

The initial condition is given by:

$$u = v = Z = 0, \; p = p_a \quad @ t = 0 \,, 0 < x < L \,, 0 < r < R_O \tag{30}$$

that corresponds to static isothermal oxidized only conditions.

3. NUMERICAL METHODOLOGY

The Finite Volume Method was used to discretize the governing equations (2)-(5), with a collocated grid arrangement, and the WUDS (Weighted Upstream Differencing Scheme) interpolation scheme, in a structured mesh. Grid is numerically generated by the solution of a partial differential equations system. The SIMPLEC (Semi-Implicit Method for Pressure Linked Equations-Consistent) algorithm is employed to address the pressure-velocity coupling.

Initially a grid convergence study was conducted considering the limiting case without irregularities. The examined meshes were 40x40, 80x80 and 160x160 volumes. The streamlines and temperature profiles obtained with the three meshes were compared. According to the gains on results in relation to the simulation computational time, the 80x80 grid was selected for the present study.

Besides the grid convergence study, code validation using numerical (Xu and Smooke, 1993) and experimental (Mitchell et al, 1980) literature data was also performed. Results show that we cannot reproduce the experimental results in their entirety behavior. A necessary condition is the chemical reactions treatment considering finite rate and more sophisticated reaction mechanisms. However, the model can estimate the temperature field, the flame position and its height, and the molar fractions of the chemical species in the complete combustion of the hydrocarbon in a satisfactory way. The detailed validation procedure and its results are shown in (Leitão, 2017) and (Sauer, 2012).

4. RESULTS

In order to explore the results, a base case is initially established. From the base case, a parametric study is conducted to evaluate the effects on the recirculation zones and the flame shape of the position and the size of the irregularities, of buoyancy and of the Reynolds number of the fluid flow. The base case operational conditions are shown in Tab. 1.

Table. 1. Base case conditions

Geometric Parameters	$R_O = 2.54\ cm$	$R_F = 6.35\ mm$	$L = 30\ cm$
Operational conditions	Fuel Side @ $0 < r < R_F,\ x = 0$	Air Side @ $R_F < r < R_O,\ x = 0$	
Axial input velocity	$u_F = 4.5\ cm/s$	$u_O = 9.88\ cm/s$	
Radial input velocity	$v_F = 0\ cm/s$	$u_O = 0\ cm/s$	
Mass fraction	$Y_{CH_4} = 1.0$	$Y_{O_2} = 0.232,\ Y_{N_2} = 0.768$	
Input temperature	$T_{in} = 298\ K\ @\ 0 < r < R_O,\ x = L$		
Output pressure	$p_{out} = 1.0\ atm\ @\ 0 < r < R_O,\ x = L$		
Chemical reaction	$CH_4 + 2(O_2 + 3.76N_2) \rightarrow CO_2 + 2H_2O + 7.52N_2$		
Reynolds number	$\mathrm{Re} = 2R_O u_O \rho / \mu = 317.6$		
Gravity	$g = 9.81$ m/s (Axial direction; opposite to the fluid flow)		
Wavy wall model	$R_w(x) = R_O - P \cdot e^{\frac{-(x-H)^2}{\sigma}}\ @\ 0 < x < L$		
Wavy wall geometric parameters	$H = 0.25L$	$P = 0.50R_O$	$\sigma = 5 \cdot 10^{-4}$

Figure 2 shows the difference in the temperature field, streamlines and flame shape between the base case and the limit case without irregularities. For better visualization, the results are plotted for a complete section of the burner, although the governing equations are solved in an axissimetric domain.

The flame presents an over-ventilated behavior for both cases. For the base case (Fig. 2a), immediately upstream of the irregular wall peak, the oxidant-rich flow deflects in the centerline direction, deforming the flame, and decreasing flame height ($h_f = 9\ cm$) when compared to the case without irregular wall ($h_f = 9.25\ cm$) (Fig. 2b). This reduction in the flame height is related to the improvement in oxidant transport, due to enhanced convective effects by the irregular wall for the base case.

Besides the change in the radial velocity that affects the flame upstream of the irregularity peak, an increase of the axial velocity along the centerline is also observed, due to the reduction in the transversal area imposed by the irregular wall.

An increase in the recirculation zone downstream of the irregular wall peak is also observed due to the wall irregularity that induces the flow separation. Under conditions of absence of gravitational forces, axial convective effects are reduced. Buoyancy force accelerates the high temperature gases in the axial direction, lengthening the flame.

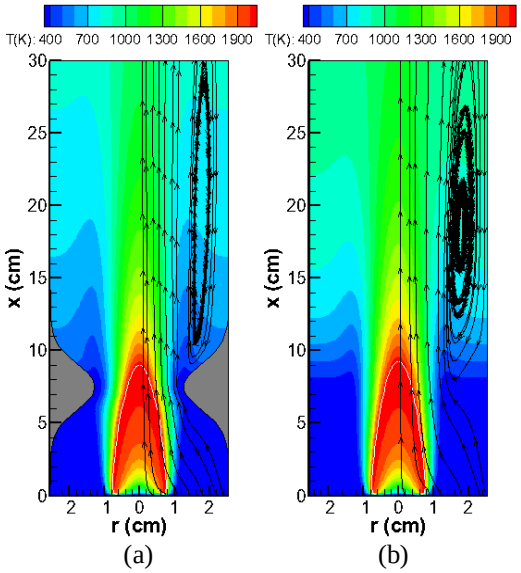

Figure 2. (a) Base case; (b) Case without irregularities. Temperature field, streamlines in black (shown only in half domain) and flame shape in white.

In order to evaluate the buoyancy effects on flame and flow field parameters, in Fig. 3, zero gravity acceleration (g) simulations were conducted from the cases shown in Fig. 2. Gravitational effects are responsible for the entry of cold external air near the solid wall, generating or intensifying recirculation zones, a characteristic that can be observed comparing Fig. 2b with Fig. 3b. Thus, in the absence of gravitational effects, the over-ventilated flame width increases for the referred case with and without irregularities, as shown in Fig. 3a and Fig. 3b.

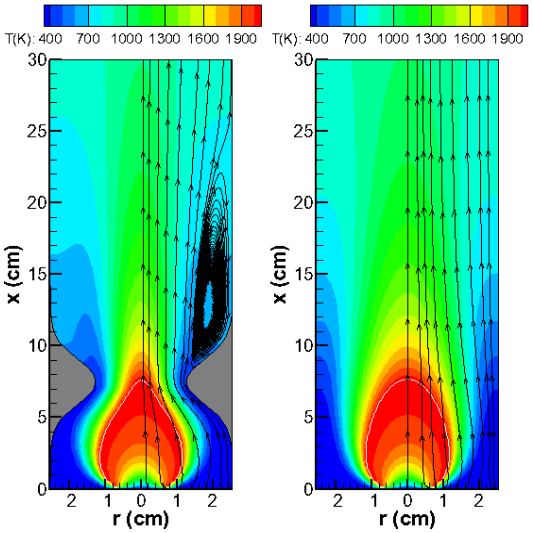

Figure 3. (a) Base case nullifying the gravitational force; (b) Case without irregularities nullifying the gravitational force. Temperature field, streamlines in black (shown only in half domain) and flame shape in white.

The influence of the number of peaks was also studied trough, simulations considering two undulations in the irregular wall. The undulations peaks were positioned at the axial positions $H = 0.25L$ and $H = 0.125L$. The parameter σ was changed to $1 \cdot 10^{-4}$ so the decay of the Gaussian function that models the irregular wall is more pronounced. The results are shown in Fig. 4.

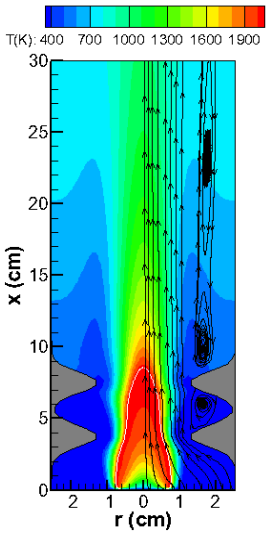

Figure. 4. Two undulations wall. Temperature field, streamlines in black (shown only in half domain) and flame shape in white.

The inclusion of more undulations peaks, when compared to the base case (Fig. 2a), generate new recirculation zones, downstream of the undulations. Flame shape is affected upstream of the peak of each undulation as oxidant is deflected towards the channel centerline. Figure. 4 ($h_f = 8.56\ cm$) shows a stronger flame deflection connected with the irregular surface peak closer to injection than the deflection in a higher axial position. The existence of larger radial

velocities in the region upstream of the undulation closer to injection as compared to the radial velocities upstream of the other undulation as observed from the streamline shapes in Fig. 4 is responsible for this effect.

The influence of the irregularity position it was also investigated through changes in the parameter H from the original value ($H = 0.25L$) to the conditions of $H = 0.125L$ and of $H = 0.5L$. The results are shown in Fig. 5.

For the case with $H = 0.125L$ ($h_f = 8.35\ cm$) (Fig. 5a), the flame height is 7% lower than the base case ($h_f = 9.0\ cm$) (Fig. 2a). The flame deflection occurs in a lower axial position associated with the oxidant deflection. The recirculation zone is formed in a lower axial position due to the irregularity new position, which induces the flow separation closer to the injection surface.

For the case with $H = 0.5L$ ($h_f = 9.26\ cm$) (Fig. 5b), the flame height is 3% higher than the base case. Two recirculation zones are observed for this irregularity position, one upstream of the irregularity caused by buoyancy effects, and another one downstream of the irregularity, caused by both buoyancy effect and solid wall shape that induces the fluid flow separation downstream of the peak of the irregular wall (see Fig. 2a).

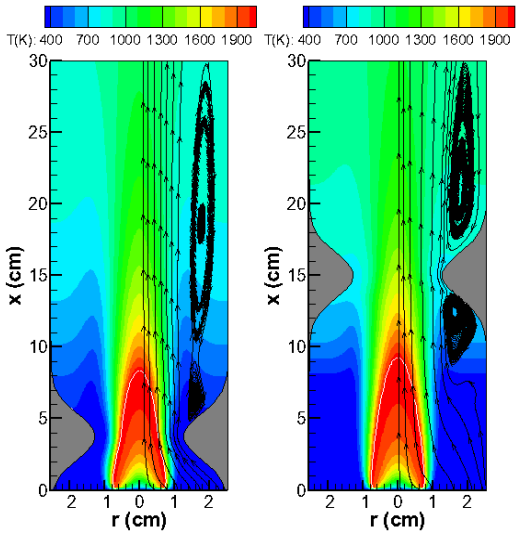

(a) (b)

Figure. 5. Irregularity position: (a) $H = 0.125L$; (b) $H = 0.50L$. Temperature field, streamlines in black (shown only in half domain) and flame shape in white.

The irregularity height effect was also investigated changing the parameter P from the original value ($P = 0.5R_O$) to the conditions of $P = 0.25R_O$ and of $P = 0.65R_O$. The results are shown in Fig. 6. For the case with $P = 0.25R_O$ (Fig. 6a), it is verified that the flame reaches an intermediate height ($h_f = 9.2\ cm$) between the value obtained in the base case ($h_f = 9.0\ cm$) (Fig. 2a) and the case without irregularities ($h_f = 9.25\ cm$) (Fig. 2b). Decreasing the irregularity size reduces the deflection of the oxidant-rich stream flow towards the domain centerline direction, leading an increase the flame height.

For the case with $P = 0.65R_O$ (Fig. 6b), it is observed an opposite trend. Increasing the irregularity size, it is raised the deflection of the oxidant-rich flow towards in the centerline direction, decreasing the flame height ($h_f = 8.73\ cm$) for a fixed irregularity position.

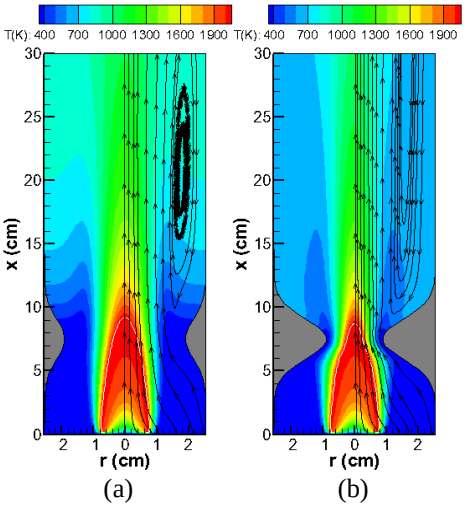

Figure. 6. Irregularity size: (a) $P = 0.25R_O$; (b) $P = 0.65R_O$. Temperature field, streamlines in black (shown only in half domain) and flame shape in white.

Finally, the effect of the Reynolds number is investigated by changing the oxidant axial inlet velocity. Then, to evaluate the influence of the Reynolds number, it is changed, in the case shown in Fig. 5b, the original value of u_O (see Tab.1) to conditions of $\mathrm{Re} = 500$ ($u_O = 15.55\ cm/s$) and of $\mathrm{Re} = 150$ ($u_O = 4.66\ cm/s$). The results are shown in Fig. 7.

Increasing the Reynolds number of the flow (Fig. 7a), the oxidant flow increases, providing a larger amount of oxidant, forcing the flame surface to achieve a smaller height ($h_f = 9.2\ cm$) when compared to the similar case with the original Reynolds number (Fig. 5b).

Comparing the temperature fields in Fig. 5b and Fig. 7a, we observe that a larger amount of oxidant entering at low temperature affects the temperature throughout the entire domain, decreasing it, in a fixed axial position. This larger amount of oxidant also changes the convection intensity, modifying the position of the recirculation zone downstream of the irregularity position, which is formed in a higher axial position. The area of the recirculation zone is also modified, caused by the fluid separation induced by the irregular wall shape itself. The recirculation zone became much less intense with a bigger area extrapolating the solution domain.

Decreasing the Reynolds number of the flow (Fig. 7b), the oxidant flow rate is decreased, so the amount of oxidant will be insufficient for the complete combustion of the fuel. The flame presents an under-ventilated behavior ($h_f = 6.58\ cm$), expanding into the solid walls. In this case, two recirculation zones are formed, one upstream of the irregularity caused by the buoyancy effect, and another one downstream of the irregularity, caused by solid wall shape that induces the fluid flow separation downstream of the peak of the irregular wall.

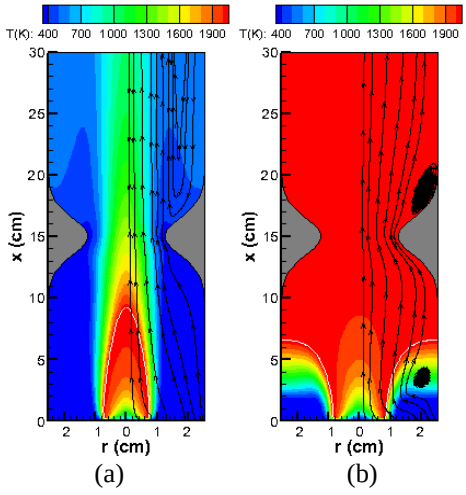

Figure. 7. Reynolds number: (a) $\mathrm{Re} = 500$; (b) $\mathrm{Re} = 150$. Temperature field, streamlines in black (shown only in half domain) and flame shape in white.

5. CONCLUSIONS

In the present study, we conducted an analysis of a reactive flow confined in a cylindrical tube in the presence of irregular walls. A parametric study was conducted to evaluate the effects on the recirculation zones and the flame shape of the position and the size of the irregularities, of buoyancy and of the Reynolds number of the fluid flow.

The irregularity affects the flame shape inside the tube. Increasing the irregularity maximum height or positioning the irregularity closer to the reagent inlets, the over-ventitlated flame height decreases. Also, gravitational effects are shown to narrow and to stretch the flame.

Recirculation zones are formed near the reagent inlets due to buoyancy effects, and just downstream of the irregularity, caused by solid wall shape that induces the fluid flow separation. In some cases, these two recirculation zones are shown to coalescence into a single flow structure. The variation in the number of Reynolds of the flow affects directly in the temperature field, in the recirculation zones position and in the flame behavior: over- or under- ventilated configuration.

6. ACKNOWLEDGEMENTS

The authors would like to thank the PRH-37 program “Mechanical Engineering for the Efficient Use of Biofuels” of the Brazilian Petroleum Agency (ANP), CNPq – Brazilian Council for Development of Science and Technology and FAPERJ – Carlos Chagas Filho Foundation for Research Support of the State of Rio de Janeiro – for financial support.

7. REFERENCES

Ansari, M. and Amani, E., 2018. “Micro-combustor performance enhancement using a novel combined baffle-bluff configuration”. *Chemical Engineering Science*, Vol. 176, No. 16, pp. 243–256.

Burke, S.P. and Schumann, T.E.W., 1928. “Diffusion flames”. *Industrial & Engineering Chemistry*, Vol. 20, No. 10, pp. 998–1004.

García, A., M., Rendon, M., A. and Amel, A., A., 2020. “Combustion model evaluation in a CFD simulation of a radiant-tube burner”. *Fuel*, Vol. 276, Article 118013.

Kanury, A., M., 1982. *Introduction to Combustion Phenomena*, Gordon and Breach, New York, USA, p. 411.

Leitão, R., J., 2017. *Escoamentos Reativos de Jatos Concorrentes Laminares na Presença de Ondulações*, M.Sc. thesis, Universidade Federal do Rio de Janeiro, Rio de Janeiro, Brasil.

Mitchell, R., Sarofim, A. and Clomburg, L., 1980. “Experimental and numerical investigation of confined laminar diffusion flames”. *Combustion and Flame*, Vol. 37, pp. 227–244.

Nascimento, V., P., 2005. *Escoamentos Reativos Laminares na Presença de Obstruções em Canais de Placas Paralelas*, M.Sc. thesis, Universidade Federal do Rio de Janeiro, Rio de Janeiro, Brasil.

Ortiz, F., J., G., 2011. “Modeling of fire-tube boilers”. *Applied Thermal Engineering*, Vol 31, No. 16, pp. 3463-3478.

Pan, J., Zhang, C., Pan, Z., Wu, D., Zhu, Y., Lu, Q. and Zhang, Y., 2020. “Investigation on the effect of bluff body ball on the combustion characteristics for methane/oxygen in micro combustor”. *Energy*, Vol. 190, Article 116465.

Sauer, V. M., 2012. *Análise de Escoamentos Reativos de Biocombustíveis em Dutos*. M.Sc. thesis, Universidade Federal do Rio de Janeiro, Rio de Janeiro, RJ, Brazil.

Shilong, Z. and Yuxin, F., 2020. “Experimental and numerical study on the flame characteristics and cooling effectiveness of air-cooled flame holder”. *Energy*, Vol. 209, Article 118421.

Wan, J. and Zhao, H., 2020. “Effect of thermal condition of solid wall on the stabilization of a preheated and holder-stabilized laminar premixed flame”. *Energy*, Vol. 200, Article 117548.

Wan, J., Wu, Y. and Zhao, H., 2020. “Excess enthalpy combustion of methane-air in a novel micro non-premixed combustor with a flame holder and preheating channels”. *Fuel*, Vol. 271, Article 117518.

Williams, F.A., 1994. *Combustion Theory: Second Edition*. Westview Press, second edition.

Xu, Y. and Smooke, M., D., 1993. “Application of a primitive variable newton’s method for the calculation of an axisymmetric laminar diffusion flame”. *Journal of Computational Physics*, Vol. 104, No. 1, pp. 99–109.

8. RESPONSIBILITY NOTICE

The authors are the only responsible for the printed material included in this paper.